Journal of Solid State Chemistry 187 (2012) 244–248

Contents lists available at SciVerse ScienceDirect

Journal of Solid State Chemistry

journal homepage: www.elsevier.com/locate/jssc

The hydrogenation of Dy_5Pd_2 followed by *in situ* methods

H. Kohlmann [a,*], E. Talik [b], T.C. Hansen [c]

[a] Inorganic Solid State Chemistry, Saarland University, Am Markt, Zeile 3, 66125 Saarbrücken, Germany
[b] Institute of Physics, University of Silesia, Uniwersytecka 4, 40-007 Katowice, Poland
[c] Institut Laue-Langevin, 6, Rue Jules Horowitz, BP 156, 38042 Grenoble Cedex 9, France

ARTICLE INFO

Article history:
Received 26 September 2011
Received in revised form
6 January 2012
Accepted 15 January 2012
Available online 24 January 2012

Keywords:
In situ techniques
Thermal analysis
Metal hydrides
Dysprosium hydride
Hydrogenation

ABSTRACT

The hydrogenation behavior of the intermetallic compound Dy_5Pd_2 was investigated by means of *ex situ* X-ray powder diffraction, *in situ* neutron powder diffraction and *in situ* differential scanning calorimetry. The structural model of Dy_5Pd_2 with a palladium atom at the 32(e) position x, x, x ($x \approx 0.22$, 7/8 occupation) and a dysprosium atom at almost the same location ($x \approx 0.18$, 1/8 occupation) is confirmed. Upon heating the latter approaches x(Pd) and at $T=399$ K both positional parameters are indistinguishable. Dy_5Pd_2 does not incorporate hydrogen (deuterium) into its crystal structure, however, starting at $T=495$ K reacts with hydrogen to non stoichiometric dysprosium dideuteride, DyD_{2+x}, following a parabolic rate law. *In situ* differential scanning calorimetry at various hydrogen pressures up to 2.5 MPa shows strongly exothermic signals, whose temperature onset depend on the gas pressure, corresponding to the formation of a mainly ionic hydride (DyH_{2+x}).

1. Introduction

Intermetallic compounds of dysprosium with palladium are of interest for their rich crystal chemistry and correlated electron behavior [1–3]. From the eight binary intermetallic phases in the dysprosium palladium system, Dy_5Pd_2 is the one with the lowest congruent melting point, just below 1200 K [4]. Its crystal structure could finally be solved by Fornasini in the cubic space group *Fd*-3*m* with half of the atoms occupying crystallographic sites only partially [5]: apart from half-occupation of one dysprosium site, one dysprosium atom with 1/8 occupation (32(e) x, x, x with $x=0.167$) and one palladium atom with 7/8 occupation (32(e) x, x, x with $x=0.228$) share almost the same location. According to these crystallographic properties the true composition of "Dy_5Pd_2" using site multiplicities and occupancies is rather $Dy_{48+32/2+32*1/8}Pd_{32*7/8}=Dy_{68}Pd_{28}=Dy_{4.857}Pd_2=Dy_{2.429}Pd=Dy_{2.125}Pd_{0.875}$; however, for reasons of simplicity and conformity to former literature, this compound will still be called Dy_5Pd_2 in the following text. Despite this kind of disorder in Dy_5Pd_2, no homogeneity range was detected in any of the compounds M_5Pd_2 (M=Y, Tb, Dy, Ho, Er, Tm, Lu [5]) crystallizing in this structure type and being its only representatives. The similarity to the Ti_2Ni type structure has already been discussed by Fornasini [5], which in turn can be described either as a stuffed senarmontite (cubic Sb_2O_3) type or a defect variant of the structure types of W_3Fe_3C, W_6Fe_6C, Co_2W_4C or M_3Ti_3O (M=Mn, Fe, Co, Ni, Cu) [6].

Dy_5Pd_2 shows complex electrical transport and magnetic properties [7], which might be influenced by the incorporation of interstitial hydrogen atoms. Furthermore, a possible hydrogen uptake of intermetallic palladium compounds such as Dy_5Pd_2 would be interesting in view of the nature of the chemical bond in a possible hydride, because ternary hydrides of palladium are extremely versatile as for their chemical bonding, crystal structures and compositions. Alkaline earth palladium hydrides, for example, may be either semiconductors exhibiting 18-electron hydridometallate complexes with covalent palladium–hydrogen interactions [8–11] or metallic compounds with interstitial hydrogen [12–15], depending on the composition.

We have therefore undertaken a study on the hydrogenation behavior of Dy_5Pd_2. Only one such hydrogenation study on a compound with Dy_5Pd_2 type structure has been reported as yet, i.e., Er_5Pd_2. This, however, was only investigated at hydrogen pressures 1 mbar $\leq p(H_2) \leq$ 1000 mbar (101 Pa $\leq p(H_2) \leq$ 101 kPa) and temperatures 473 K $\leq T \leq$ 1148 K, where decomposition to binary erbium hydride and the palladium richer intermetallic phases Er_3Pd_2, ErPd and Er_3Pd_4 was observed [16]. We have now attempted hydrogenation reactions on Dy_5Pd_2 and at considerably higher pressures than previously performed on the homologous erbium compound and followed the reactions by *in situ* methods to allow for intermediate phases to be detected.

Experiments have been carried out using both the natural isotopic mixture of hydrogen (differential scanning calorimetry)

* Corresponding author. Fax: +49 681 302 70652.
E-mail address: h.kohlmann@mx.uni-saarland.de (H. Kohlmann).

0022-4596/$ - see front matter © 2012 Elsevier Inc. All rights reserved.
doi:10.1016/j.jssc.2012.01.029

and isotopic pure deuterium (neutron powder diffraction). Only for the latter the two cases will be clearly denoted, while for general discussions the terms hydrogen, hydride and hydrogenation are used in a generic way for both cases. This is justified, because isotope effects are generally small enough to not affect the conclusions drawn here. For a more detailed discussion of isotope effects in metal hydrides and other hydrogenous materials see references [17,18].

2. Experimental details

2.1. Synthesis of intermetallic compounds

Ingots of Dy_5Pd_2 were obtained from the starting materials Dy (99.9% purity) and Pd (Specpure Johnson Matthey Chemical Ltd.) which were melted together in stoichiometric amounts (molar ratio $n(Dy)/n(Pd)=68/28$) on a water-cooled eight-segment conical coil with diameter 14 mm in stoichiometric amounts under very pure argon atmosphere in a Czochralski apparatus [19]. The obtained ingots were remelted several times to homogenize them. The RF electromagnetic field causes a levitation of the melt, conducting the electric current much better than oxides, which collect on a surface of the bottom part of a melt drop. Moreover, the strong stirring of the melt by this method ensures homogenization. No significant evaporation of the melt during the crystal growth was observed. The ingots were ground to powders with a silver luster, which were not sensitive to air.

2.2. In situ neutron powder diffraction (NPD)

Neutron powder diffraction data of Dy_5Pd_2 were taken *in situ* under various deuterium (isotopic purity 99.8%) gas pressures up to 2.5 MPa at the Institute Laue-Langevin in Grenoble, France, at $T=299(1)$ K on the high intensity powder diffractometer D20 in high resolution mode (average resolution $\Delta d/d=3\times10^{-3}$) in the range $3^\circ\leq2\theta\leq150^\circ$ (0.1° step width in 2θ) with a time resolution of 4 min per pattern. Deuterium was used in order to avoid the strong incoherent scattering of the ^{1}H (protium) isotope of hydrogen. For a detailed discussion of isotope effects in metal hydrides and hydrogenous materials in general and with regard to neutron diffraction see references [17,18]. The sample was placed inside a single crystal sapphire based gas pressure cell especially designed for *in situ* neutron powder diffraction [14]. The deuterium gas pressure was varied by a gas pressure controller during the measurements and the sample was heated using a contactless laser heating system. The pyrometer was calibrated against the lattice parameter of palladium refined from neutron diffraction data using the same sapphire gas pressure cell. The temperature dependence of palladium's lattice parameter was taken from [20]. The neutron wavelength used was determined from a measurement on a NIST 640b silicon standard to be $\lambda=186.71(1)$ pm and kept fixed during refinements. Rietveld refinements were carried out with the program FULLPROF [21] and pseudo-Voigt as profile function. Refined structural parameters are listed in Table 1 of the Supplementary Material.

2.3. X-ray powder diffraction (XRPD)

XRPD data were collected using flat transmission samples containing an internal silicon standard on an image plate Guinier powder diffractometer (Huber Guinier camera G670 at $T=296(1)$ K with Cu$K_\alpha1$ radiation, $\lambda=154.056$ pm). Rietveld refinements were carried out with the program FULLPROF [21] and pseudo-Voigt as profile function.

2.4. In situ thermal analysis (DSC)

Differential scanning calorimetry was performed *in situ* under hydrogen pressures of up to 2.5 MPa and temperatures up to 700 K on a Q1000 DSC (TA Instruments) equipped with a gas pressure chamber. 20–30 mg of the powdered intermetallics were put in aluminum crucibles, which were closed with an aluminum lid. These were placed inside the pressure chamber, which was then purged several times with hydrogen gas before filling it to the desired hydrogen gas pressure. The samples were heated at a rate of 10 K/min, held at the final temperature for 1 h and cooled back to 300 K at 10 K/min. Usually, two or three such runs were performed, before the hydrogen pressure was released, the sample taken out and structural characterization undertaken. After releasing the gas pressure, the products were characterized *ex situ* by XRPD (see Section 2.3). All hydrogenated samples were handled in an argon filled glove box due to the air sensitivity of the hydrides.

3. Results and discussion

3.1. In situ neutron powder diffraction (NPD)

3.1.1. Ambient conditions

The samples were single-phase, well crystallized Dy_5Pd_2, as indicated by the X-ray and neutron powder diffraction patterns. In the case of neutron diffraction, however, neutron absorption caused by dysprosium has to be considered. Unlike for samarium and europium with a strong resonance absorption, the neutron absorption cross section of ^{nat}Dy almost obeys the $1/v$ law for thermal neutrons and shows much lower absorption cross sections than the former two [22]. Still, the absorption effect on the neutron powder pattern is appreciably and the use of high flux neutron diffractometers such as D20 [23] is very important in such a case. Strategies for dealing with strong absorbers in neutron powder diffraction using constant wavelength thermal neutrons have been described before [24–28].

In the *in situ* neutron powder diffraction experiment, the Dy_5Pd_2 sample has been subjected to 2.5 MPa deuterium pressure and then heated slowly with two laser beams (Fig. 1). For the structural refinements the structural model of Fornasini was taken with isotropic thermal displacement parameters and occupational parameters fixed to literature values [5], but an overall temperature factor was refined. As can be seen from Fig. 1 broad signals show up especially during heating, which could be attributed to phonon scattering of the sapphire single crystal [14,29]. Therefore, the range $52^\circ\leq2\theta\leq58$ was excluded from refinements (shaded area in Fig. 1). Refined positional and lattice parameters for Dy_5Pd_2 at ambient conditions differ from the published data [5] by less than three times the combined standard uncertainties (compare to Table 1 in Supplementary Material). The structure model of Fornasini can thus be confirmed on the basis of these NPD data.

3.1.2. Section (a): Heating to $T=495$ K at $p(D_2)=2.5$ MPa

The variation of the lattice parameter a of Dy_5Pd_2 with temperature (Fig. 2) is similar to that of the same compound at low temperatures ($T<300$ K [7]). While the positional parameters x(Dy1), x(Dy2) and x(Pd) are almost constant upon heating, x(Dy3) is approaching the value of x(Pd) (Fig. 3). The difference between these two positional parameters decreases from 7 times the combined standard uncertainties at room temperature to less than 1 at $T=399$ K. Therefore, from this temperature on, positional parameters of Dy3 and Pd are constrained to be of the same value. This behavior may point at one of two scenarios: (1) At

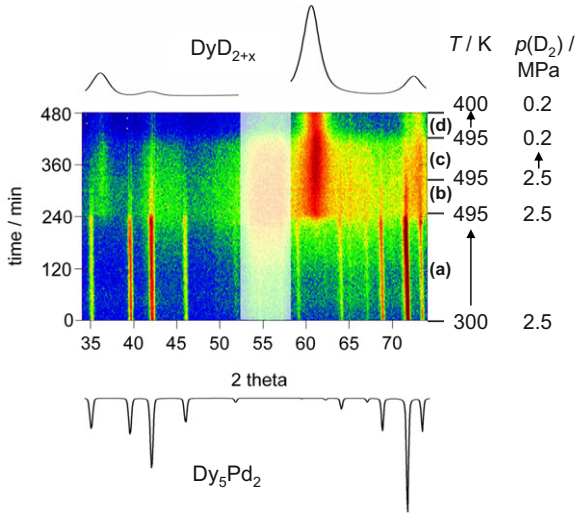

Fig. 1. *In situ* neutron powder diffraction data of the deuteration of Dy_5Pd_2 taken on the neutron powder diffractometer D20 [23] at $\lambda=186.71(1)$ pm in a single crystal sapphire gas pressure cell [14] under various deuterium gas pressure and temperature conditions, intensities in false color. The range $52^\circ \le 2\theta \le 58$ (shaded area) was excluded from refinements due to (temperature dependent) scattering from the sapphire single crystal. Section (a) corresponds to heating, (b) to keeping at constant reaction conditions, (c) to lowering gas pressure and (d) to lowering the temperature. Bottom and top show calculated neutron powder diffraction patterns for the starting (Dy_5Pd_2) and final deuteration product (DyD_{2+x}) for comparison with the *in situ* data.

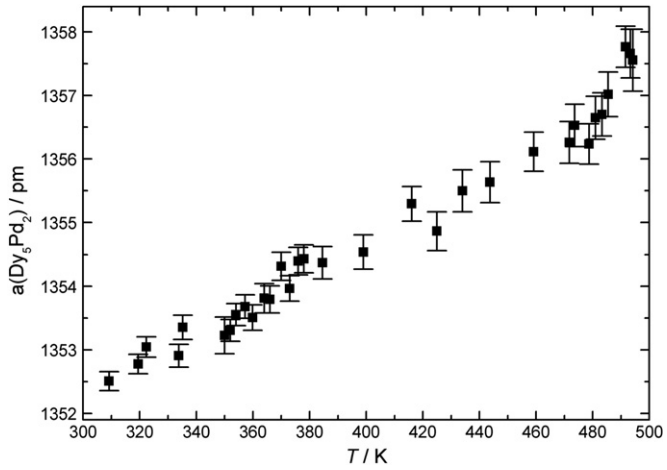

Fig. 2. The lattice parameter a of Dy_5Pd_2 as a function of the temperature at $p(D_2)=2.5$ MPa as determined from *in situ* neutron powder diffraction. Error bars correspond to estimated standard uncertainties. All numerical values are listed in Table 1 of the Supplementary Material.

higher temperatures disordering phenomena take place. (2) With the increased thermal displacement at higher temperatures, the two atomic positions become indistinguishable; especially the Dy3 position, which is only occupied to 1/8, is difficult to locate from such powder diffraction data at elevated temperatures. Further investigations will be necessary to clarify this point. There is no sign of deuterium incorporation into the crystal structure of Dy_5Pd_2 up to a temperature of $T=495$ K. At this point a reaction of Dy_5Pd_2 with deuterium takes place.

3.1.3. *Section (b): Holding at T=495 K and p(D2)=2.5 MPa*

At $T=495$ K and $p(D2)=2.5$ MPa deuterium pressure very broad new diffraction lines appear (Fig. 1), which could be indexed on the basis of a cubic unit cell. They were assigned to binary dysprosium

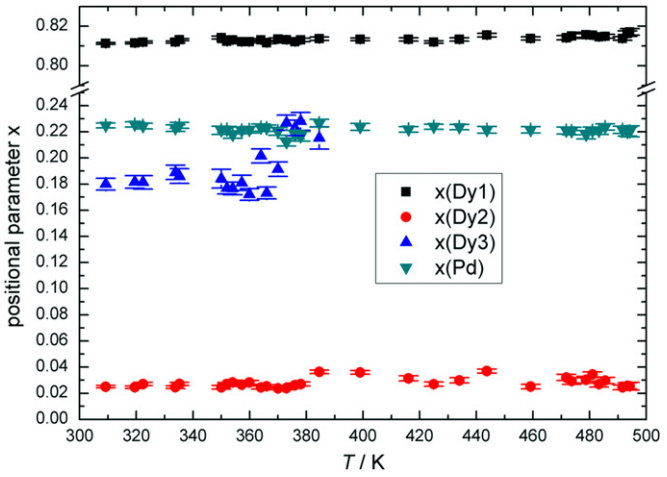

Fig. 3. Positional parameters of Dy_5Pd_2 as a function of the temperature at $p(D_2)=2.5$ MPa as determined from *in situ* neutron powder diffraction. Error bars correspond to estimated standard uncertainties. All numerical values are listed in Table 1 of the Supplementary Material.

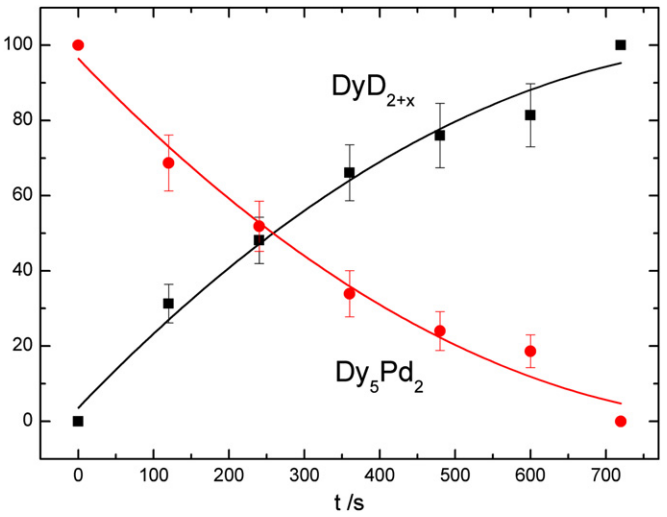

Fig. 4. Phase fractions of Dy_5Pd_2 (red circles) and DyD_{2+x} (black squares) as a function of time at $T=495$ K and $p(D_2)=2.5$ MPa as derived from Rietveld refinements (only crystalline phases considered), with fit according to a parabolic rate law. Error bars correspond to estimated standard uncertainties.

deuteride DyD_{2+x} with a lattice parameter of $a=520$ pm. DyD_{2+x} was reported to crystallize in a fluorite like structure, i.e., deuterium occupies all tetrahedral voids in a cubic closest packing of dysprosium atoms, with the additional x deuterium atoms in octahedral interstices. This arrangement is stable up to $x=0.18$ for the deuteride [30]. The refined lattice parameters suggest the composition to be close to DyD_2 with $x=0$ (compare to $a(DyD_2)=519$ pm [31]), however, the occupation of deuterium in octahedral voids is significant according to Rietveld refinements on the NPD data. While keeping $T=495$ K and $p(D2)=2.5$ MPa deuterium pressure for 12 min, neither the lattice parameter of Dy_5Pd_2 ($a=1357.5(4)$ pm) nor that of DyD_{2+x} ($a=520.6(3)$ pm) vary significantly. The growth of DyD_{2+x} at the expense of Dy_5Pd_2 follows a parabolic rate law (Fig. 4), typical for diffusion controlled solid–gas reactions [32]. Dy_5Pd_2 has been completely consumed within 10 min in a deuterium-induced decomposition to binary dysprosium deuteride with very poor crystallinity (very broad reflections, Figs. 1 and 4). No further diffraction lines are present, i.e., any other phase is diffraction amorphous.

3.1.4. Sections (c) and (d): Lowering pressure and temperature

After the reaction came to a halt, first the pressure and then the temperature was reduced to ambient. In the course of this change the cubic lattice parameter increases to $a=522.0(2)$ pm at $T=321$ K and $p(D_2)=101$ kPa. According to the well-known fact that for most non-stoichiometric lanthanide dihydrides lattice parameters are inversely proportional to the hydrogen content [33–35], this behavior points at a lower deuterium content at ambient conditions.

3.2. In situ differential scanning calorimetry (DSC)

The hydrogenation of Dy_5Pd_2 was also followed by *in situ* thermal analysis. The reaction commences between room temperature and 350 K, depending on the hydrogen gas pressure (Figs. 5–7), and exhibits a strong exothermic signal on the first heating cycle. This is typical for the formation of an ionic hydride from an intermetallic compound. The position of the exothermic signal can be lowered to smaller temperatures by raising the hydrogen pressure. The second cycles run immediately after the first one without opening the sample chamber do not show this exothermic signal, indicating that the hydrogenation of Dy_5Pd_2 was already finished after cycle one. However, reversible effects with maxima at about 430 K and 460 K are recorded, for 0.5 MPa and 1.4 MPa hydrogen gas pressure (Figs. 5 and 6), respectively, as endothermic signals upon heating in the second cycle and with a slight hysteresis as exothermic signals upon cooling in the second cycle. These effects may be attributed to further hydrogen de- and absorption depending on temperature, and are probably outside the recorded temperature range for the data set at 2.5 MPa hydrogen gas pressure (Fig. 7). After returning the samples to ambient conditions, the products were characterized by *ex situ* X-ray powder diffraction. For a hydrogenation at 0.3 MPa hydrogen pressure and 400 K only very broad reflections of binary DyH_2 could be recognized in the diffraction pattern. Products of the reaction at 0.5 MPa and 500 K still show poorly crystalline DyH_2, however, alongside with small amounts of $PdH_{0.7}$. Hydrogenations at $p(H_2)=1.4$ MPa and $T=700$ K finally yields the phases DyH_2, DyH_{2+x}, DyH_3 and $PdH_{0.7}$, all with a moderate crystallinity. For hydrogenation at $p(H_2)=2.5$ MPa and $T=500$ K, mimicking the conditions of the *in situ* NPD experiments (see Section 3.1), again binary dysprosium hydride and small amounts of binary palladium hydride was the reaction product, the latter in a very poorly crystalline state as evidenced by very broad XRD reflections. The absence of these broad reflections of palladium hydride (deuteride) in the *in situ* NPD patterns may be due to the fact that palladium with a bound coherent scattering length $b_c=5.9$ fm is a much weaker scattering nucleus as compared to dysprosium with $b_c=16.9$ fm.

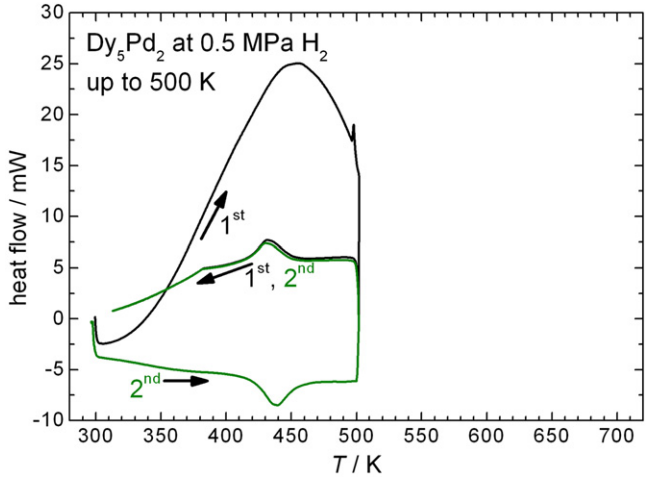

Fig. 5. *In situ* DSC of the hydrogenation of Dy_5Pd_2 at 0.5 MPa hydrogen pressure, showing strong exothermic signals upon the first heating cycles. Heating and cooling rates 10 K/min. First and second denote first and second cycle of the measurement on the same sample.

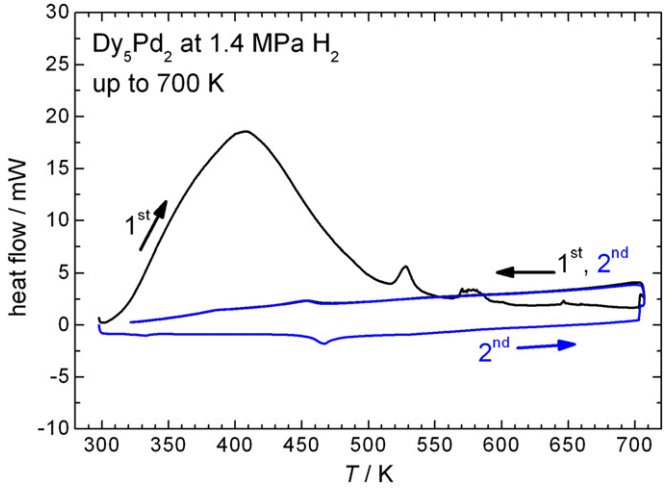

Fig. 6. *In situ* DSC of the hydrogenation of Dy_5Pd_2 at 1.4 MPa hydrogen pressure, showing strong exothermic signals upon the first heating cycles. Heating and cooling rates 10 K/min. 1st and 2nd denote first and second cycle of the measurement on the same sample.

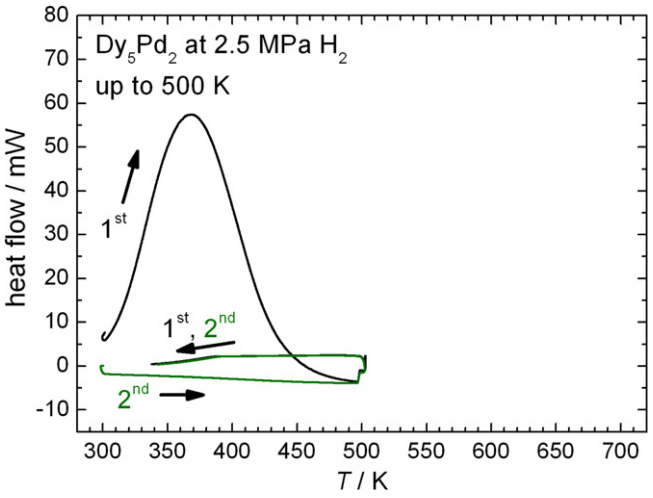

Fig. 7. *In situ* DSC of the hydrogenation of Dy_5Pd_2 at 2.5 MPa hydrogen pressure, showing strong exothermic signals upon the first heating cycles. Heating and cooling rates were matched to reaction conditions of the *in situ* NPD experiment. First and second denote first and second cycle of the measurement on the same sample. Note the higher heat flow as compared to Figs. 5 and 6 due to doubled sample mass.

4. Conclusion

The cubic crystal structure of Dy_5Pd_2 could be confirmed by neutron powder diffraction. Upon heating the free positional parameter x(Dy3) approaches the value of x(Pd), i.e., the positions of Dy3 (1/8 occupation) and Pd (7/8 occupation) become indistinguishable at $T \geq 399$ K. Both X-ray and neutron powder diffraction do not show evidence for a ternary Dy–Pd hydride, but rather prove that Dy_5Pd_2 decomposes to binary hydrides upon hydrogenation. *In situ* NPD gives a detailed picture of the hydrogenation

reaction. Halting at $T=495$ K and $p(D_2)=2.5$ MPa yields the formation of DyD_{2+x}, which follows a parabolic rate law typical for diffusion controlled solid–gas reactions. The surplus x deuterium atoms are located in octahedral voids of the fluorite like arrangement of the binary deuteride. Exothermic signals of *in situ* DSC experiments up to 2.5 MPa and 700 K confirm the formation of binary DyH_{2+x} upon hydrogenation of Dy_5Pd_2. The hydrogenation behavior of Dy_5Pd_2 is thus different from that of Eu_5Pd_2. While the latter forms binary EuH_2 and Eu_2PdH_4 with a complex 18-electron tetrahydridopalladate anion upon hydrogenation [9], the former yields binary hydrides of its constituents dysprosium and palladium. Up to now, no ternary rare earth palladium hydrides have been reported except for europium and ytterbium.

Appendix A. Supplementary information

Supplementary data associated with this article can be found in the online version at doi:10.1016/j.jssc.2012.01.029.

References

[1] G.R. Stewart, Rev. Mod. Phys. 73 (2001) 797–855.
[2] G.R. Stewart, Rev. Mod. Phys. 78 (2006) 743–753.
[3] O. Loebich Jr., E. Raub, J. Less-Common Met. 39 (1973) 47–62.
[4] Z. Du, H. Yang, Y. Xu, J. Alloys Compd. 302 (2000) 199–203.
[5] M.L. Fornasini, A. Palenzona, J. Less-Common Met. 38 (1974) 77–82.
[6] B.G. Hyde, S. Anderson, Inorganic Crystal Structures, John Wiley & Sons, New York, 1989.
[7] M. Klimczak, E. Talik, J. Kusz, W. Hofmeister, A. Winiarski, R. Troc, Mater. Sci.Pol. 25 (2007) 263–267.
[8] W. Bronger, J. Alloys Compd. 229 (1995) 1–9.
[9] H. Kohlmann, H.E. Fischer, K. Yvon, Inorg. Chem. 40 (2001) 2608–2613.
[10] K. Yvon, Metal hydrides: transition metal hydride complexes, in: K.H.J. Buschow, R.W. Cahn, M.C. Flemings, B. Ilschner, E.J. Kramer, S. Mahajan (Eds.), Encyclopedia of Materials: Science and Technology, Elsevier, Amsterdam, 2004, pp. 1–9.
[11] H. Kohlmann, Z. Kristallogr. 224 (2009) 454–460.
[12] E. Rönnebro, D. Noréus, M. Gupta, K. Kadir, B. Hauback, P. Lundqvist, Mater. Res. Bull. 35 (2000) 315–323.
[13] H. Kohlmann, G. Renaudin, K. Yvon, C. Wannek, B. Harbrecht, J. Solid State Chem. 178 (2005) 1292–1300.
[14] H. Kohlmann, N. Kurtzemann, R. Weihrich, T. Hansen, Z. Anorg. Allg. Chem. 635 (2009) 2399–2405.
[15] H. Kohlmann, Z. Kristallogr. 225 (2010) 195–200.
[16] S. Ramaprabhu, A. Weiss, Ber. Bunsen Ges. 93 (1989) 146–156.
[17] M.T. Weller, P.F. Henry, V.P. Ting, C.C. Wilson, Chem. Commun. (2009) 2973–2989. (Cambridge, U. K.).
[18] V.P. Ting, P.F. Henry, H. Kohlmann, C.C. Wilson, M.T. Weller, Phys. Chem. Chem. Phys. 12 (2010) 2083–2088.
[19] E. Talik, J. Szade, J. Heimann, A. Winiarska, J. Winiarski, A. Chelkowski, J. Less-Common Met. 138 (1988) 129–136.
[20] B.N. Dutta, B. Dayal, Status Solidi B 3 (1963) 2253–2259.
[21] J. Rodriguez-Carvajal, FullProf.2k, Version 3.70 – Jul2006-ILL JRC, 2006, unpublished.
[22] J.E. Lynn, P.A. Seeger, At. Data Nucl. Data Tables 44 (1990) 191–207.
[23] T.C. Hansen, P.F. Henry, H.E. Fischer, J. Torresgrossa, P. Convert, Meas. Sci. Technol. 19 (2008) 034001.
[24] K. Yvon, H. Kohlmann, B. Bertheville, Chimia 55 (2001) 505–509.
[25] H. Kohlmann, B. Bertheville, T. Hansen, K. Yvon, J. Alloys Compd. 322 (2001) 59–68.
[26] H. Kohlmann, R.O. Moyer Jr., T. Hansen, K. Yvon, J. Solid State Chem. 174 (2003) 35–43.
[27] H. Kohlmann, F. Werner, K. Yvon, G. Hilscher, M. Reissner, G.J. Cuello, Chem. Eur. J. 13 (2007) 4178–4186.
[28] H. Kohlmann, Eur. J. Inorg. Chem. (2010) 2582–2593.
[29] G.J. McIntyre, H. Kohlmann, B.T.M. Willis, to be published.
[30] T.J. Udovic, Q. Huang, J.W. Lynn, R.W. Erwin, J.J. Rush, Phys. Rev. B: Condens. Matter 59 (1999) 11852.
[31] I.N. Goncharenko, V.P. Glazkov, O.A. Lavrova, V.A. Somenkov, Sov. Phys. Solid State 34 (1992) 1585–1586.
[32] H. Schmalzried, Solid State React., Solid State Phenom. 56 (1997) 13–36.
[33] G.G. Libowitz, Nonstoichiometry in metal hydrides, in: Nonstoichiometric Compounds, Adv. Chem. Ser. 1963, pp. 74–86.
[34] M. Chiheb, J.N. Daou, P. Vajda, Z. Phys. Chem. (Muenchen, Ger.) 197 (1993) 255–260.
[35] P. Vajda, G. André, J. Hammamm, Phys. Rev. B: Condens. Matter 55 (1997) 3028–3032.